Proc. Natl. Acad. Sci. USA
Vol. 94, pp. 13927–13931, December 1997
Medical Sciences

Polyclonal structure of intestinal adenomas in $Apc^{Min}/+$ mice with concomitant loss of Apc^{+} from all tumor lineages

A. J. MERRITT*†, K. A. GOULD*‡§, AND W. F. DOVE*‡¶

*McArdle Laboratory for Cancer Research and ‡Laboratory of Genetics, University of Wisconsin, Madison, WI 53706

Communicated by Eric S. Lander, Whitehead Institute for Biomedical Research, Cambridge, MA, October 20, 1997 (received for review August 19, 1997)

ABSTRACT **When tumors form in intestinal epithelia, it is important to know whether they involve single initiated somatic clones. Advanced carcinomas in humans and mice are known to be monoclonal. However, earlier stages of tumorigenesis may instead involve an interaction between cells that belong to separate somatic clones within the epithelium. The clonality of early tumors has been investigated in mice with an inherited predisposition to intestinal tumors. Analysis of Min (multiple intestinal neoplasia) mice chimeric for a ubiquitously expressed cell lineage marker revealed that normal intestinal crypts are monoclonal, but intestinal adenomas frequently have a polyclonal structure, presenting even when very small as single, focal adenomas composed of at least two somatic lineages. Furthermore, within these polyclonal adenomas, all tumor lineages frequently lose the wild-type *Apc* allele. These observations can be interpreted by several models for clonal interaction within the epithelium, ranging from passive fusion within regions of high neoplastic potential to a requirement for active clonal cooperation.**

Studies of cellular interactions are important to the fundamental understanding of the process of tumorigenesis, particularly in epithelia. Early studies have indicated that colonic adenomas and carcinomas are monoclonal in carcinogen-treated mice (1, 2) and in humans (3). A recent study of familial colon cancer in humans by Novelli and colleagues (4) described adenomas of mixed karyotype in a mosaic XY ↔ XO human male with familial adenomatous polyposis (FAP). The authors suggested that adenoma formation involves cooperation between cells and that monoclonality arises later by outgrowth of a dominant clone. An alternative interpretation raised by the authors is that the mixed karyotype arose by loss of the Y chromosome after adenoma formation, because the patient carried an unstable dicentric Y chromosome.

FAP patients carry a germ-line mutation in the *APC* (adenomatous polyposis coli) gene. Adenoma formation is usually associated with a second, somatic, *APC* mutation. The study by Novelli *et al*. (4) did not address whether each lineage within the polyclonal adenomas incurred somatic mutation or loss of the wild-type *APC* allele. The authors favored a hypothesis in which an *APC*-negative clone induced dysplasia in adjacent *APC*-heterozygous cells. Indeed, in a more recent study of nonmosaic FAP individuals, Bjerknes and colleagues (5) reported that early adenomas frequently contain both APC-positive and APC-negative dysplastic crypts.

Min mice are heterozygous for a germ-line mutation in *Apc*, the mouse homolog of the human *APC* gene (6). Like FAP patients, Min mice on the C57BL/6J (B6) background develop numerous adenomatous polyps throughout the small and large intestine (7). In these mice, adenoma formation is associated with extensive loss of the wild-type allele of *Apc*, apparently through chromosome loss (8). Previously we have analyzed mice chimeric for the *Min* mutation and the ubiquitously expressed cell lineage marker *ROSA26* (9, 10). We found that the neoplastic component of the adenomas was derived solely from the $Apc^{Min}/+$ component (11). Because the *Min* mutation was present in only one component of these chimeras, we were not able to analyze the clonality of the tumors. Here, we describe studies of chimeras in which both the *ROSA26* component and the non-*ROSA26* component carry the *Min* mutation of *Apc*.

MATERIALS AND METHODS

Mouse Strains. $Apc^{Min}/+$ mice were bred and housed at the McArdle Laboratory and were used after 36 generations of backcrossing to B6 (B6-Min), obtained from The Jackson Laboratory. The *ROSA26* marker was carried by males homozygous for *ROSA26* at the 8th backcross (N_8) F_1 generation on the B6 background. We have found that the fertility of B6 males is compromised by homozygosity for *ROSA26* in N_{10} congenic strains, but fortunately it was retained in the N_8 males used in these experiments.

Generation and Genotyping of Chimeras. Chimeras were generated by morula aggregation as described in Hogan *et al.* (12). To produce *ROSA26*/+ $Apc^{Min}/+$ ↔ +/+ $Apc^{Min}/+$ chimeras, single embryos produced by a B6-Min × B6-*ROSA26*/*ROSA26* cross were aggregated with those produced by a B6 × B6-Min cross. The genotypes of the chimeras were determined by quantitative PCR for the *Min* region of the *Apc* locus (13). At 90 days of age, mice were sacrificed by CO_2 asphyxiation. Normal intestinal tissue was dissected from the proximal, middle, and distal small intestine and from the large intestine of the chimeras and of control B6-Min animals. The preparation of DNA (11) and the PCR assay for the ratio of Apc^{+} to Apc^{Min} alleles (8) have been described previously. Ratios of Apc^{Min}/Apc^{+} from the chimeras were not significantly different from those from nonchimeric Min controls ($P > 0.05$; Wilcoxon rank sum test).

Serial Sectioning and Genotyping of Adenomas from Chimeras. Intestines from chimeras were fixed flat in 0.2% glutaraldehyde for 30 min and then stained overnight with

Abbreviations: *APC*/*Apc*, the adenomatous polyposis coli gene of the human/the mouse; B6, the C57BL/6J inbred mouse strain; DSI, distal small intestine; FAP, familial adenomatous polyposis; LI, large intestine; Min/*Min*, the mouse strain exhibiting multiple intestinal neoplasia, owing to the *Min* mutation of *Apc*; MSI, middle small intestine; N, backcross generation; PSI, proximal small intestine; *ROSA26*, reverse orientation splice acceptor site β-galactosidase/neomycin resistance fusion gene insertion no. 26; X-Gal, 5-bromo-4-chloro-3-indolyl β-D-galactopyranoside.

†Present address: Department of Epithelial Biology, Paterson Institute, Wilmslow Road, Manchester, M20 9BX, United Kingdom.
§Present address: Department of Biochemistry, University of Wisconsin, Madison, WI 53706.
¶To whom reprint requests should be addressed at: McArdle Laboratory for Cancer Research, University of Wisconsin, 1400 University Avenue, Madison, WI 53706. e-mail: dove@oncology.wisc.edu.

The publication costs of this article were defrayed in part by page charge payment. This article must therefore be hereby marked "*advertisement*" in accordance with 18 U.S.C. §1734 solely to indicate this fact.

5-bromo-4-chloro-3-indolyl β-D-galactopyranoside (X-Gal) as previously described (13). Tumors were then postfixed in 10% formalin overnight, embedded in paraffin, serially sectioned through the entire adenoma, and counterstained with nuclear fast red. The sections were then examined for evidence of polyclonality. The X-Gal stain was found to have a limited penetration distance (13) and, therefore, for some of the larger adenomas clonality was judged from the outer edges of the adenomas. Adenomatous regions from histological sections were scraped and genotyped for the *Min* allele and *D6Mit36* as previously described (8, 13).

Immunohistochemistry for Apc. The rabbit polyclonal antibody 3122 was a generous gift from Carol Midgely and David Lane, University of Dundee, Scotland, and was used at a dilution of 1/450 in a standard peroxidase-based protocol. Briefly, 5-μm adenoma sections were dewaxed and rehydrated through a graded ethanol series. Antigen retrieval was performed by microwaving the slides in citrate buffer (pH 6) for 25 min on full power in a 650-W Kenmore microwave. Endogenous peroxidase activity was quenched by incubation of the slides in 0.3% hydrogen peroxide for 15 min at room temperature. Immunohistochemistry was then performed with the ABC *elite* peroxidase system according to the manufacturer's directions (Vector Laboratories, Burlingame, CA). Sections were developed in diaminobenzidine substrate (Sigma) with 0.01% nickel chloride. Sections were weakly counterstained with nuclear fast red for 30 sec. The 3122 antibody recognizes amino acids 13–352 of the human APC polypeptide, a region that is proximal to the *Min* mutation and, therefore, would be present in the truncated Apc polypeptide produced by the Apc^{Min} allele. The lack of staining of the Min adenomas may be the result of a conformational change whereby the antigen is obscured. Although carboxyl-terminal Apc antibodies are available, the fixation condition required for the X-Gal staining was incompatible with the use of those antibodies in this study (A.J.M., unpublished observations). Apc expression observed with 3122 is located in the apical cytoplasm of normal intestinal tissue and increases from the base to the top of the crypt, consistent with other reports using different antibodies (14).

RESULTS

Generation and Characterization of Chimeras. To test whether adenomas commonly consist of multiple cell lineages, we generated aggregation chimeras in which both lineages were heterozygous for the Apc^{Min} mutation and only one lineage carried the *ROSA26* marker (9, 10). ROSA26 constitutively expresses β-galactosidase and has been demonstrated to be a stable cell lineage marker for both normal and neoplastic murine intestinal tissue (13, 14). The parental strains used to generate the chimeras were extensively backcrossed to B6. The resulting uniform B6 background minimized the influence of unlinked segregating modifier loci that could affect the Min phenotype (15). Adenomas from these chimeras were analyzed for polyclonal composition and presence of the wild-type *Apc* allele.

Following X-Gal staining of whole-mount intestinal tissue, we observed two mice that developed adenomas within both the blue (*ROSA26*/+) and white (+/+) lineages. This observation indicated that both lineages were heterozygous for the Apc^{Min} mutation. Normal intestinal tissue from these mice was confirmed to be of the *ROSA26*/+ Apc^{Min}/+ ↔ +/+ Apc^{Min}/+ genotype by quantitative PCR for the Apc^{Min} mutation (8).

Whole-mount intestinal preparations of these two chimeras revealed 8.2:1 and 9.6:1 ratios of white to blue tissue, as determined by quantitative PCR for *D6Mit36*, a simple sequence length polymorphism (SSLP) marker closely linked to the *ROSA26* insertion site (13). (This ratio of white to blue tissue was not characteristic of all chimeras examined. Among 39 *ROSA26*/+ ↔ +/+ chimeras examined by Gould and Dove (13) and in this study, we observed a broad spectrum of ratios of white to blue.) A high degree of mixing of the two lineages was observed with a mean patch diameter of six crypts for the minority blue (*ROSA26*/+) lineage. All normal crypts from both the small and large intestines of the chimeras were monoclonal. The villi, which are composed of cells supplied from six to eight crypts (see ref. 16), were of mixed lineage at patch boundaries, as reported previously (17).

Histological Examination of Adenomas. Initial examination of the whole-mount intestines under a dissecting microscope revealed that, from a total of 260 adenomas in the two chimeric animals, 229 appeared to be pure white, 13 pure blue, and 18 mixed blue/white. To examine the apparently mixed tumors more closely, we performed a more detailed analysis by serial sectioning (Table 1). Examination of sections revealed that 5 of the 18 apparently mixed adenomas were actually tight clusters of individual blue and white adenomas, separated by the border of normal cells that surrounds Min adenomas (13). Of the 13 adenomas classified as pure blue in the whole-mount preparations, 8 were found to be mixed when examined in serial sections. In addition, one of 10 randomly chosen adenomas classified as pure white in the whole mounts was found to be mixed. Each of these mixed adenomas appeared to be a single focal adenoma, containing adjacent sectors of *ROSA26*/+ and +/+ lineages (Fig. 1). Some adenomas contained multiple lineage boundaries, with several blue and white sectors within an

Table 1. Distribution of pure and mixed adenomas within the intestines of *ROSA26*/+ Apc^{Min}/+ ↔ +/+ Apc^{Min}/+ chimeras

		Number of intestinal adenomas			
Chimera	Intestinal region	Mixed blue/white	Pure blue	Pure white	Total
112	PSI	0	0	9	9
	MSI	2	1	24	27
	DSI	4	4	53	61
	LI	1	0	7	8
	Total	7	5	93	105
113	PSI	3	1	24	28
	MSI	4	0	55	59
	DSI	6	0	60	66
	LI	2	0	0	2
	Total	15	1	139	155

The numbers of pure blue and mixed adenomas were determined from detailed serial section analysis. The composition of each of a sample of 10 overtly pure white adenomas was assessed by analysis of serial sections, whereas the remaining pure white adenomas were scored from whole-mount analysis only. For both chimeric mice the entire small and large intestines were scored. LI, large intestine; PSI, proximal small intestine; MSI, middle small intestine; DSI, distal small intestine.

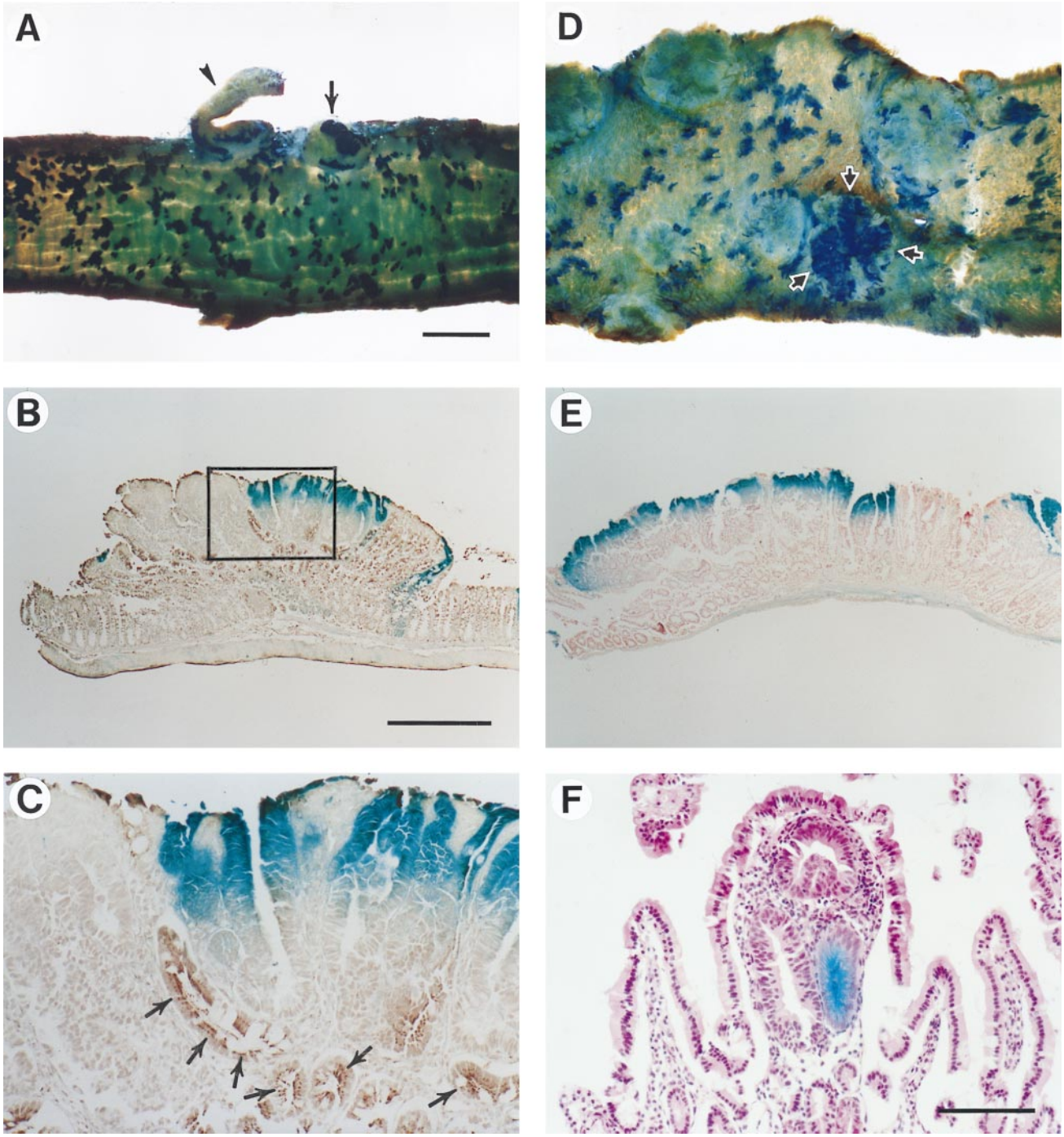

FIG. 1. Whole-mount preparations, histological sections, and Apc immunohistochemistry of polyclonal intestinal adenomas. (*A*) Whole-mount preparation of the large intestine from chimera 113 after X-Gal staining, showing blue and white patches in the chimeric normal intestine and two adenomas, both of which contain both blue and white components. The arrow points to adenoma 5983, the arrowhead points to adenoma 5984 (see Table 2). (*B*) Histological section (5 μm) of adenoma 5983 stained with Apc antibody 3122. The box represents a region where blue and white regions join. (*C*) A $\times$4 magnification of the box in *B* showing a blue Apc-negative adenoma region on the right, a white Apc-negative adenoma region on the left, and normal Apc-positive crypts at the bottom (arrows). (*D*) Whole-mount preparation of the middle small intestinal region from chimera 113 after X-Gal staining; several white adenomas are present and one mixed blue/white adenoma, 6003, delineated by three arrows. (*E*) Histological section (5 μm) of adenoma 6003 stained with nuclear fast red. A blue adenoma region is observed on the left and a white adenoma region on the right. (*F*) A polyclonal microadenoma from the small intestine of chimera 113 stained with hematoxylin and eosin. (Scale bars = 2 mm for *A* and *D*, 0.5 mm for *B* and *E*, and 0.1 mm for *F*.)

apparently single adenoma. Individual dysplastic crypts within mixed adenomas were always of a single lineage.

Overall, there were 22 mixed adenomas, confirmed by histological analysis, out of 260 (Table 1), giving a frequency of 6.7% for chimera 112 and 9.7% for chimera 113, or 8.5% overall. This observed frequency of mixed adenomas is likely to be an underestimate of the actual frequency of polyclonal adenomas. Many overtly pure adenomas may involve more than one clone, but this cannot be ascertained when the different clones carry the same marker. Further, because we were unable to perform the detailed histological analysis on all the white adenomas, more of these may actually be mixed. Because the blue component is the minority contribution for each chimera, a lower limit estimate of 79% for the frequency of polyclonal adenomas can be derived from the

frequency of adenomas with any blue contribution that are mixed in lineage [22 overtly mixed/(22 overtly mixed + 6 pure blue)]. This value is consistent with the high frequency estimated by Novelli *et al.* (4).

Analysis of the Status of the *Apc* Locus. Bjerknes and colleagues (5) observed that within FAP adenomas only a fraction of dysplastic crypts lose wild-type APC expression. This observation prompted us to examine the Apc^+ status of the polyclonal adenomas in our chimeras. We performed quantitative PCR for the *Min* region of *Apc* (8) on DNA isolated from both blue and white sectors of eight mixed adenomas: five of the eight mixed adenomas showed extensive loss and the rest showed at least marginal loss of the marker for the wild-type *Apc* allele in both lineages (Table 2). These results indicate that loss of Apc^+ is frequently associated with adenoma formation in all lineages of polyclonal tumors.

A more complete analysis of the *Apc* status of these adenomas requires histochemistry. We examined by immunoperoxidase assays the distribution of Apc protein in the mixed adenomas. Sections from 22 mixed adenomas were stained with the Apc antibody 3122 according to a modified peroxidase protocol. Nine samples were unscorable owing to excess tissue damage incurred during the immunohistochemistry. Normal crypts within the epithelium adjacent to adenomas were Apc-positive and served as an internal positive control (Fig. 1). In all 13 adenomas, both the +/+ and the *ROSA26*/+ sectors were Apc-negative (Fig. 1, Table 2). Adenomas from nonchimeric B6-Min mice also failed to stain with this antibody (A. R. Shoemaker and A.J.M., unpublished data). These results demonstrate that all lineages within polyclonal adenomas lose Apc^+ expression. Thus, our results differ from the observation that in an FAP adenoma only a subset of dysplastic crypts lose APC^+ expression (5).

Hypotheses for the Origin of Mixed Adenomas. Several hypotheses must be considered for the origin of the mixed adenomas: random collision between tumors, somatic mosaicism for the *ROSA26* marker, epigenetic silencing of ROSA26 expression, and interaction between multiple initiated clones. We have found evidence against each of these classes of hypotheses except that of interaction between clones.

(i) *Random collision*. Owing to the large number of adenomas in these chimeras it is expected that some random collisions between distinct tumors will occur. Novelli *et al.* (4) calculated that such collisions could not explain the number of mixed tumors that they observed. In our study, collision tumors appeared as mixed in the whole-mount preparations, but they were reclassified as multiple separate tumors when assessed in serial histological sections and were excluded from the polyclonal category. In addition, mixed adenomas were found in regions of low adenoma multiplicity, where collisions would be unlikely to occur. For example, in the entire large intestine of chimera 113, there were only two adenomas, and both were mixed (Fig. 1, Table 1). Mixed tumors were not always large. For example, a small, <0.5 mm, microadenoma consisting of only three dysplastic crypts but of mixed lineage was observed in the small intestine (Fig. 1*F*). These observations suggest that random collision of individual tumors is unlikely to account for all the mixed tumors observed.

(ii) *Mosaicism within the adenoma*. Another possibility is that the mixed adenomas arose from a *ROSA26*/$^+$ adenoma that had secondarily lost the region on chromosome 6 that contains the *lacZ* insertion site, producing *ROSA26*/+ ↔ 0/+ mosaic tumors. This model is highly unlikely because sectored adenomas have never been observed in histological sections of tumors from nonchimeric *ROSA26*/+ Min mice or in chimeras that carry the Apc^{Min} mutation only on the *ROSA26*/+ lineage (13).

(iii) *Epigenetic silencing of* ROSA26 *expression*. This explanation is also highly unlikely because of the absence of white sectoring in nonchimeric *ROSA26*/+ Min mice. To investigate the possibility that *ROSA26* is somatically silenced in the white sectors of mixed adenomas, we examined the status of the

Table 2. Characterization of sectors of mixed adenomas for *Apc* and *ROSA26* status

Adenoma	Intestinal region	Mean Apc^+/Apc^{Min} ratio*		LOH at *Apc* Locus		No. of sectors	Apc immunostaining, no. of Apc-negative sectors/total tested	Mean *D6Mit36* 129/B6 ratio	
		Blue	White	Blue	White			Blue	White
5968	LI	0.467	0.654	Marginal	Marginal	5	5/5	0.554	0.113
5976	DSI	ND	ND	ND	ND	3	3/3	0.900	0.162
5978	DSI	ND	ND	ND	ND	2	2/2	ND	ND
5983	LI	ND	ND	ND	ND	3	2/2	0.828	0.058
5984	LI	ND	ND	ND	ND	2	2/2	0.705	0.033
5992	MSI	0.418	0.339	Marginal	Marginal	3	2/2	0.631	0.045
5996	DSI	0.359	0.164	Marginal	Extensive	2	ND	0.671	0.014
5997	DSI	0.226	0.178	Extensive	Extensive	3	3/3	0.808	0.038
5999	DSI	0.198	0.243	Extensive	Extensive	3	2/2	0.903	0.038
6000	DSI	ND	ND	ND	ND	2	2/2	ND	ND
6001	DSI	0.171	0.125	Extensive	Extensive	4	2/2	0.770	0.025
6003	MSI	0.115	0.117	Extensive	Extensive	3	ND	0.983	0.025
6006	MSI	ND	ND	ND	ND	4	3/3	1.075	0.031
6013	PSI	0.276	0.286	Extensive	Extensive	4	2/2	0.771	0.043
6015	PSI	ND	ND	ND	ND	2	2/2	ND	ND

DNA was prepared separately from the blue and white adenoma regions of mixed adenomas. Loss of the Apc^+ allele was determined by the methods of Luongo *et al.* (8). Ratios of Apc^+/Apc^{Min} of <0.3 were described as having extensive Apc^+ loss and those of >0.3 as marginal loss. These ratios were compared with the ratio for normal intestinal tissue from Min mice: 1.12 ± 0.15. The allelic ratio values were corrected for the larger size of the Apc^{Min} product relative to the Apc^+ product by multiplying the Apc^{Min} value by 0.85. In the study by Luongo *et al.* (8), 100% of B6-Min adenomas showed extensive Apc^+ loss. The marginal values described here may reflect normal cell contamination due to the increased difficulty of scraping tissue from very small tumor regions within the mixed adenomas. Apc immunohistochemistry was performed on mixed adenomas with polyclonal antibody 3122. Apc negativity of a sector was registered only when the adjacent normal crypts were strongly positive. Negative control sections were incubated in the absence of the primary 3122 antibody. The total number of sectors per adenoma was assessed from multiple serial sections stained only with nuclear fast red and X-Gal. The number of sectors tested by immunostaining was not always the total number present in the adenoma because individual slides did not always contain all of the sectors in a tumor. Genotype at the *D6Mit36* locus linked to *ROSA26* was determined as previously described (13), and ratios between the 129 and B6 alleles were generated. All individual ratios for both the *Apc* and *ROSA26* assays represent a mean of at least two values found to be within 0.1 of the mean. Intestinal regions abbreviated as in Table 1; LOH, loss of heterozygosity.

tightly linked simple sequence length polymorphism (SSLP) marker *D6Mit36*. In all 12 mixed tumors analyzed, the blue adenomatous regions were heterozygous for *D6Mit36*, whereas the white adenomatous regions lacked the 129/Sv allele (Table 2). A faint signal from the 129/Sv allele was observed in some of the white adenoma sectors and probably corresponds to contamination by normal stromal tissue of the other *ROSA26* genotype (13). These results confirm that the white regions of the mixed adenomas were *ROSA26*-negative in genotype and were not a result of the silencing of *ROSA26*-positive regions.

(iv) *Polyclonality by the interaction between multiple initiated clones*. We suggest that mixed adenomas cannot be explained by random collision, by mosaicism, or by epigenetic silencing. Furthermore, they do not involve interaction between *Apc*-negative and *Apc*-heterozygous clones. We conclude that these adenomas involve interaction between multiple initiated clones, each of which has lost the wild-type *Apc* allele. Possible modes of interaction are discussed below.

DISCUSSION

The question of the polyclonality of intestinal tumors has generated apparently conflicting answers. Using X chromosome mosaicism, Fearon and his colleagues (3) observed monoclonality for 15 sporadic and 15 familial intestinal adenomas in humans. Because that study analyzed only 15 familial adenomas, it may have missed detecting the mixed class. Even if polyclonality is common, this class would be rare if the patch size of mosaics is large. As further pointed out by Fearon *et al.* (3), monoclonality may have been established by clonal dominance during tumor growth; the adenomas analyzed in these early studies were 3–4 mm in diameter. By contrast, Novelli and his colleagues (4) observed a 5% incidence of mixed adenomas in their unique X0 ↔ XY mosaic FAP patient. The observations reported here are consistent with those of Novelli *et al.* (4) and do not involve alternative interpretations considered by these authors: that mixed tumors involved Y chromosome mosaicism within the tumor or recruitment of cells carrying the wild-type allele.

The investigations reported here do not address the question of sporadic tumors. Using X-inactivation mosaicism, Griffiths *et al.* (2) observed monoclonality in 32 chemically induced intestinal tumors in mice. Ponder and Wilkinson (1) observed monoclonality in 55 chemically induced intestinal neoplastic foci. The studies of Ponder and Wilkinson (1) and Griffiths *et al.* (2) addressed the issue of patch size either by analyzing tumors arising on patch borders (1) or by calculating the patch size (2). We must be cautious in extrapolating from chemically induced to sporadic tumors, however, owing for instance to the tissue damage that may accompany chemical carcinogenesis.

If polyclonality is limited to familial adenomas, a cause may lie in the enhanced susceptibility of the neonatal intestine to tumor induction (18). There is strong evidence that normal intestinal crypts of the neonatal mouse are polyclonal (16), but they undergo a crypt purification process converting them to monoclonality by approximately 2 weeks of age. It has also been shown that somatic treatment of B6-Min mice with *N*-ethyl-*N*-nitrosourea (ENU) preferentially induces adenomas between 5 and 14 days of age (18). Thus, adenomas in B6-Min mice may be initiated preferentially in polyclonal crypts.

Several modes of interaction could explain our estimated high frequency of adenomas with polyclonal structure. One model involves passive polyclonality. If two or more *Apc*-loss events occur, each producing an Apc-negative clone, the clones are able to fuse early in tumor growth, producing a tumor of polyclonal structure. Under this hypothesis, the high frequency of mixed adenomas estimated in this study would be inconsistent with the idea that *Apc*-negative clones arise at random within the epithelium. Instead, this passive polyclonality model requires that regions of the intestine have an increased potential for initiation. With this spatial constraint, each initiated clone is likely to lie in close proximity to at least one other initiated unit. This fusion process is distinct from collision because it involves very early clones rather than established adenomas. In this model, there is no requirement for active cooperation between initiated clones; instead, they are recruited passively.

A second interaction model involves active cooperation between multiple initiated clones. Here, a single initiated clone, alone, would not generate an adenoma. Alternatively, a single initiated clone could induce dysplastic growth in adjacent $Apc^{Min}/+$ crypts, resulting in conversion to *Apc*-negativity. In either scenario, two initiated clones are required.

The third model of interaction involves a quantitative enhancement of adenoma formation by clonal cooperation. Here, a single initiated clone could result in adenoma formation, but the growth and/or survival of the adenoma is quantitatively enhanced by each *Apc*-negative clone that can contribute to the adenoma.

One emergent challenge is to distinguish among these models for polyclonal interaction in familial intestinal cancer. A further challenge is to assess the importance of clonal interactions in sporadic tumors. In the end, learning the importance of clonal interactions may illuminate the relative risks of sporadic vs. familial intestinal cancer.

We thank L. Clipson for skilled assistance with the photography and the manuscript, Dr. K. Downs for providing fertile homozygous ROSA26 male mice, and A. Shoemaker for advice on experimental procedures. We are also grateful to Drs. R. Halberg and N. Drinkwater for critical discussions and Drs. Ilse Riegel, A. Bilger, and A. Shedlovsky for comments on the manuscript. This work was supported by Core Grant CA07075 and Research Grants CA50585 and CA63677 from the National Cancer Institute.

1. Ponder, B. A. J. & Wilkinson, M. M. (1986) *J. Natl. Cancer Inst.* **77,** 967–973.
2. Griffiths, D. F. R., Sacco, P., Williams, G. T. & Williams, E. D. (1989) *Br. J. Cancer* **59,** 385–387.
3. Fearon, E. R., Hamilton, S. R. & Vogelstein, B. (1987) *Science* **23,** 193–197.
4. Novelli, M. R., Williamson, J. A., Tomlinson, I. P., Elia, G., Hodgson, S. V., Talbot, I. C., Bodmer, F. & Wright, N. A. (1996) *Science* **272,** 1187–1190.
5. Bjerknes, M., Cheng, H., Kim, H., Schnitzler, M. & Gallinger, S. (1997) *Cancer Res.* **57,** 355–361.
6. Su, L.-K., Kinzler, K. W., Vogelstein, B., Preisinger, A. C., Moser, A. R., Luongo, C., Gould, K. A. & Dove, W. F. (1992) *Science* **256,** 668–670.
7. Moser, A. R., Pitot, H. C. & Dove, W. F. (1990) *Science* **247,** 322–324.
8. Luongo, C., Moser, A. R., Gledhill, S. & Dove, W. F. (1994) *Cancer Res.* **54,** 5947–5952.
9. Friedrich, G. & Soriano, P. (1991) *Genes Dev.* **5,** 1513–1523.
10. Zambrowicz, B. P., Imamoto, A., Fiering, S., Herzenberg, L. A., Kerr, W. G. & Soriano, P. (1997) *Proc. Natl. Acad. Sci. USA* **94,** 3789–3794.
11. Gould, K. A. & Dove, W. F. (1996) *Cell Growth Differen.* **7,** 1361–1368.
12. Hogan, B., Beddington, R., Costantini, F. & Lacy, E. (1994) *Manipulating the Mouse Embryo: A Laboratory Manual* (Cold Spring Harbor Lab. Press, Plainview, NY), 2nd Ed.
13. Gould, K. A. & Dove, W. F. (1997) *Proc. Natl. Acad. Sci. USA* **94,** 5848–5853.
14. Wong, M. H., Hermiston, M. L., Syder, A. J. & Gordon, J. I. (1996) *Proc. Natl. Acad. Sci. USA* **93,** 9588–9593.
15. Gould, K. A., Luongo, C., Moser, A. R., McNeley, M. K., Borenstein, N., Shedlovsky, A., Dove, W. F., Hong, K., Dietrich, W. F. & Lander, E. S. (1996) *Genetics* **144,** 1777–1785.
16. Schmidt, G. H., Winton, D. J. & Ponder, B. A. J. (1988) *Development* **103,** 785–790.
17. Schmidt, G. H., Wilkinson, M. M. & Ponder, B. A. J. (1985) *Cell* **40,** 425–429.
18. Shoemaker, A. R., Moser, A. R. & Dove, W. F. (1995) *Cancer Res.* **55,** 4479–4485.